sustainability

MDPI

Article

Temporal and Spatial Distribution of Cloud Water Content in Arid Region of Central Asia

Kailiang Zhao [1,2,3], Guofeng Zhu [1,2,3,*], Jiawei Liu [1,2,3], Liyuan Sang [1,3], Yinying Jiao [1,3], Xinrui Lin [1,3], Lei Wang [1,2,3], Yuwei Liu [1,3], Yuanxiao Xu [1,3], Wenhao Zhang [1,3] and Linlin Ye [1,3]

1 College of Geography and Environmental Science, Northwest Normal University, Lanzhou 730070, China
2 Lanzhou Sub-Center, Remote Sensing Application Center, Ministry of Agriculture, Lanzhou 730000, China
3 Shiyang River Ecological Environment Observation Station, Northwest Normal University, Lanzhou 730070, China
* Correspondence: zhugf@nwnu.edu.cn

Abstract: To evaluate the distribution characteristics of water vapor content (WVC), cloud liquid water content (CLWC) and cloud ice water content (CIWC) in arid areas of central Asia from 1980 to 2019 were analyzed by using average data of ERA5 in the European Centre for Medium-Range Weather Forecasts. The results show that: On the spatial scale, the WVC in the arid area of central Asia is mainly between 2 and 26 kg·m^{-2}. The area of maximum water vapor content is distributed in southwestern Kazakhstan and southwestern Tajikistan, with a maximum value of 26 kg·m^{-2}. The minimum areas are distributed in eastern Tajikistan, central Kyrgyzstan, central Tajikistan, and western Xinjiang, China, with the lowest WVC of 2 kg·m^{-2}. The maximum of CLWC areas were mainly distributed in northwest Kazakhstan, with a maximum value of 0.08 kg·m^{-2}, while the minimum areas were distributed in Tajikistan, eastern Kyrgyzstan, and northwest China, with a minimum value of 0.02 kg·m^{-2}. The maximum areas of CIWC were distributed in the north of Tajikistan and the west of Kyrgyzstan, possessing a maximum value of 0.06 kg·m^{-2}. The minimum area is distributed in the western part of Central Asia with a minimum value of 0.01 kg·m^{-2}. From 1980 to 2019, the WVC generally increased, while the annual average CIWC and CLWC appeared a downward trend.

Keywords: arid region of central Asia; WVC; CLWC; CIWV; spatio-temporal distribution

Citation: Zhao, K.; Zhu, G.; Liu, J.; Sang, L.; Jiao, Y.; Lin, X.; Wang, L.; Liu, Y.; Xu, Y.; Zhang, W.; et al. Temporal and Spatial Distribution of Cloud Water Content in Arid Region of Central Asia. *Sustainability* **2022**, *14*, 15936. https://doi.org/10.3390/su142315936

Academic Editor: Jianping Guo

Received: 16 August 2022
Accepted: 19 September 2022
Published: 29 November 2022

1. Introduction

Climate change has greatly impacted the regional economy and ecology [1]. Precipitation is a key factor affecting the water cycle and climate of the earth, and it is also the principal input parameter for the simulation of hydrological processes in the basin [2]. Water resources are some of the main factors that restrict the development of arid regions, and cloud water resources are an essential part of water resources [3]. Total and extreme values of precipitation in arid regions increase linearly with increasing global temperatures, potentially leading to an increased risk of drought and flooding [4]. The ecosystem in arid and semi-arid regions is fragile and sensitive, and climate change plays a decisive role in human survival and sustainable development in this region, which has aroused widespread concern in recent years [5]. Atmospheric water vapor is a considerable part of the atmosphere, and its content occupies an important position in daily human life. Detecting atmospheric WVC is of great significance to meteorological research, such as water vapor cycle, transport, artificial precipitation, and water resources assessment. Atmospheric WVC is an important basis for artificial water increase, and its in-depth study provides a theoretical basis for effectively utilizing atmospheric water resources [6]. Central Asia lies deep in the hinterland of Asia and Europe, and it is a typical arid and ecologically fragile region [7]. Its water resources have been affected by poor management for a long time, and the interference of human activities (such as overgrazing, over-irrigation, and

over-reclamation) has led to serious land desertification, forest degradation, and ecological deterioration [8], which has also affected the economic development of arid regions. Since the 1950s, with the large-scale development of land resources in inland arid regions, a large number of water conservancy facilities have been built to intercept and utilize surface runoff, which has led to great changes in water resources and the environment in Central Asia [9] and triggered a series of serious ecological and social-economic problems. Therefore, it is of great significance to study the cloud water resources in Central Asia's arid regions and implement the optimal control strategy with water resources as the core for improving the ecological environment in central Asia, promoting the coordinated development of society, economy, and ecology, and realize the sustainable development of the whole region.

The amount of water content in clouds not only has a vital influence on the process of cloud droplet growth as well as the formation and intensity of precipitation but also as an important parameter in numerical simulations of global climate and the study of cloud effects on climate [10]. On the basis of the reanalysis data of the National Centers for Environmental Prediction (NCEP) and Climate Forecast System Reanalysis (CFSR). The analysis of the distribution of cloud water and CIWC in the world shows that the cloud water content and CIWC are obviously influenced by the topography of the atmospheric circulation and have obvious regional features [11]. The WVC and the direction and intensity of water vapor transport can affect the whole WVC and atmospheric precipitable water (PW) and then influence the precipitation [12–14]. Qian [15] concluded that cloud water resources in the semi-arid areas of East Asia will also be affected by vertical circulation (Qian et al., 2001). Gaffen's research showed that there was a linear relationship between water vapor and surface temperature. For higher temperature cyclones, 70% of the water vapor that forms precipitation comes from water vapor already in the air, and the rest comes from the evaporation of water vapor from the surface [16]. In recent years, the global average surface temperature and atmospheric temperature below 8 km have shown an increasing trend. The change of surface and lower atmospheric temperature may affect the cloud from different angles. First of all, the increase in surface temperature will promote the evaporation of water vapor into the atmosphere. When the surface air temperature drops, evaporation will be inhibited, and the WVC will decrease, thus affecting the WVC in the atmosphere. Under the same conditions, high WVC benefits the formation of clouds, which will increase the cloud amount and water content. On the contrary, low WVC will reduce cloud water content, resulting in reducing cloud amount. Based on the above research, this paper examines the spatio-temporal distribution and characteristics of cloud water resources in the arid regions of Central Asia.

Generally, NCEP/NCAR reanalysis data, International Satellite Cloud Climatology Project (ISCCP), and Cloud-Sat data are used to study water vapor flux. However, owing to the time scale and spatial resolution limitations, it is difficult to analyze cloud water resources' spatial and temporal variability on longer time scales and few meteorological stations in Central Asia. A great number of scholars have confirmed that ECMWF reanalysis information globally or regionally had high accuracy and applicability through their studies [17]. In this paper, we use ERA5 reanalysis information at a longer time scale and higher spatial resolution, the temporal and spatial changes of cloud water content in arid regions of central Asia were quantified, the impact factors of cloud water resources on climate change were analyzed, and the potential of cloud water resources development in arid regions of Central Asia was evaluated.

2. Study Area and Method

2.1. Study Area

The arid region in central Asia (34°34′–55°43′ N, 46°48′–106°98′ E) is located in the north of Pamir-Qinghai-Tibet Plateau, south of Ural Mountain-Altai Mountain, east of the Caspian Sea and Volga River, and to Helan Mountain-Wushaoling (Figure 1). It is the widest arid region in the temperate zone in the northern hemisphere of the earth's

land [10]. Arid regions lie deeply in the hinterland of Asia and Europe, and the part of ocean air currently reaching them is low. The upper westerly belt transports weak water vapor from the distant Arctic Ocean and the Atlantic Ocean and is stopped and put up by vertical topography. The precipitation is bent on the mountains. In these mountains, snow glaciers are taken shape. The average annual rainfall in an arid area is less than 150 mm. Because there are more mountains than basins and plains, the spatial distribution is very uneven [10]. The rain of the year on the windward slope of the westerly mountain is as high as 2000 mm [17]. The amount of precipitation each year in the forest zone of the Tianshan Mountains and the Altai Mountains is 1000 mm [18]. Besides, it is less than 100 mm in the desert between the Aral Sea and Turkmenistan, Tarim Basin, Turpan Basin, and Hami Basin [19].

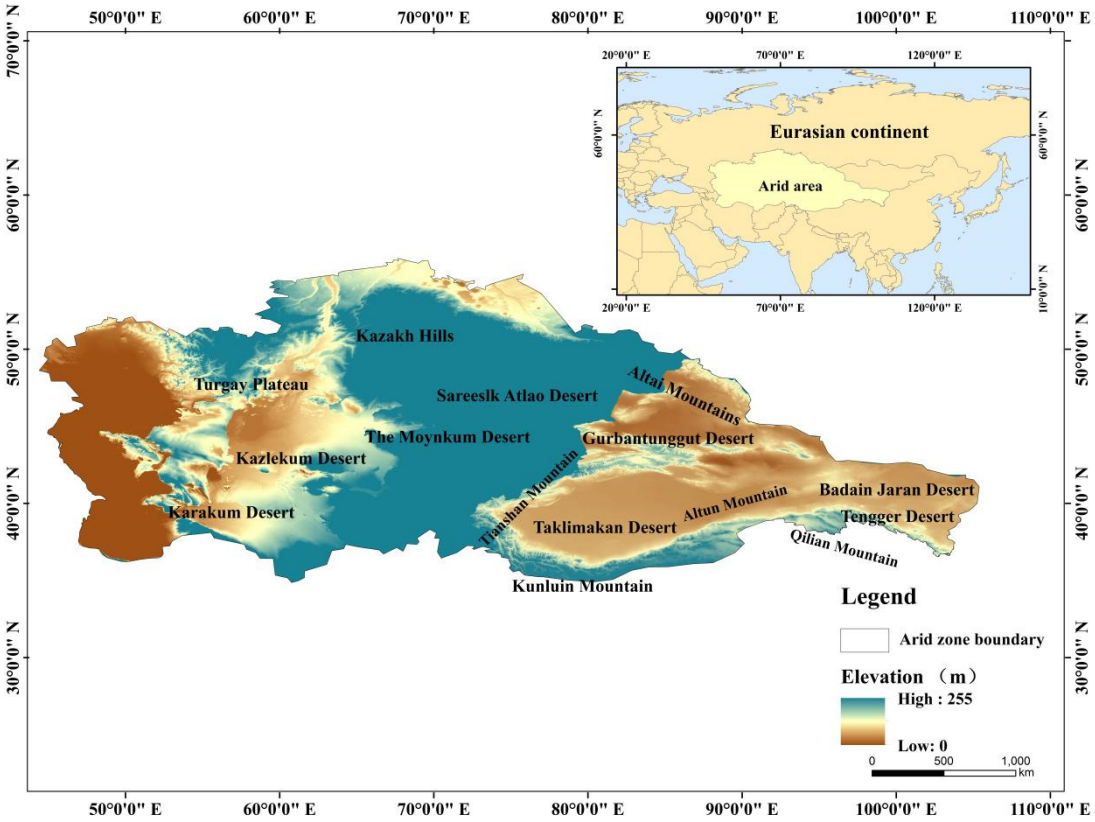

Figure 1. Central Asia Arid Zone Overview Map.

2.2. Method

In this paper, the monthly mean Total Column Water Vapor (TCWV), Cloud Liquid Water Content (CLWC), Cloud Ice Water Content (CIWC), Total Precipitation (TP), Cloud cover, and 2 m temperature of ERA5 from 1980 to 2019 were selected. The temporal resolution is hourly, and the spatial definition is 0.25° × 0.25°. The annual average distribution and the average seasonal distribution of cloud data in the central Asia arid regions were drawn using Python software. In calculation, the atmospheric WVC, CLWC, and CIWC refer to the value of each barometric layer, while the annual statistical values are calculated by the average of statistical values over the years, which are calculated by the monthly average values of each year.

The trend analysis was performed using one-dimensional linear regression analysis and least squares method to fit the slope of each raster of remote sensing images over the last 40 years to obtain the trend of multi-year values with the following equation:

$$\text{slope} = \frac{\text{n} \times \sum_{i=1}^{n} xiyi - (\sum_{i=1}^{n} xi)(\sum_{i=1}^{n} yi)}{n*\sum_{i=1}^{n} xi^2 - (\sum_{i=1}^{n} xi)^2} \quad (1)$$

where: slope is the change trend, y_i is the value of the x_ith year; when slope > 0, there is an increasing trend; when slope < 0, there is a decreasing trend.

To further evaluate the trends of WVC and cloud water content, the F-test was used to analyze the significance of the trends of the values.

3. Results

3.1. Spatial Distribution of WVC and Cloud Water Content

3.1.1. Spatial Distribution of Annual WVC

WVC is usually expressed by atmospheric Precipitable Water (PW), the amount of precipitation that can be formed when all the water vapor contained in the air column of unit value is converted into rain and snow [20]. It can be seen from Figure 2 that the WVC was mainly distributed between 2 and 26 kg·m^{-2}. Maximum areas are concentrated in southwest Kazakhstan and Tajikistan, with rich WVC, with the highest WVC, up to 24 kg·m^{-2}. The minimum regions were distributed in Tajikistan, Kyrgyzstan, and western Xinjiang, China, and the WVC was seriously deficient. They had the lowest value of 2 kg· m^{-2}.

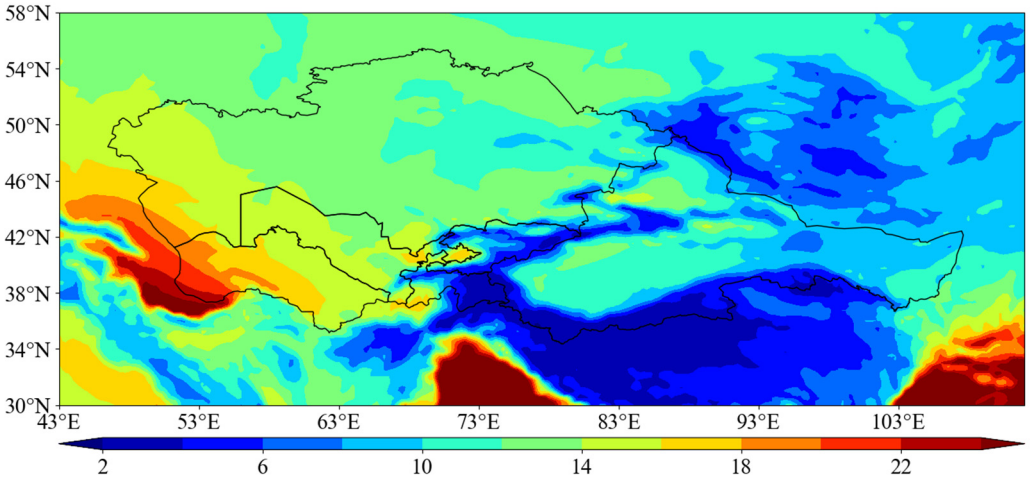

Figure 2. Spatial distribution of WVC in arid areas of Central Asia from 1980 to 2019. (Units: kg·m^{-2}).

3.1.2. Spatial Composition of Atmospheric Water Vapor in Different Seasons

From Figure 3, it can be seen that: In spring (Figure 3a), the highest value of WVC was 20 kg·m^{-2} in Turkmenistan, while the lowest value was only 2 kg·m^{-2} in Tajikistan. In summer (Figure 3b), the WVC and the high-value areas extended obviously. The high-value area was in Turkmenistan, with the maximum reaching 26 kg·m^{-2},. The values for Tajikistan and Kyrgyzstan are relatively low, with the minimum value reaching 5 kg·m^{-2}. Compared with summer, in autumn (Figure 3c), the WVC decreases, and the region of low values increases. The maximum areas were distributed in Turkmenistan, with the highest value of 27 kg·m^{-2}, while the minimum regions were distributed in Tajikistan, Kyrgyzstan, Xinjiang and Gansu, China, possessing the lowest value of only 3 kg·m^{-2}. In winter (Figure 3d), the WVC decreased significantly. The maximum area was distributed in Turkmenistan, but the highest value was 14 kg·m^{-2}, while the minimum areas were distributed in Tajikistan, Kyrgyzstan, Xinjiang, and most areas of Gansu, and the minimum value was only 1 kg·m^{-2}. On the whole, the areas with high-WVC in the arid region of central Asia were mainly distributed in parts of Turkmenistan. The high WVC was related to the proximity to the Caspian Sea. The minimum areas were mainly distributed in the arid regions of Tajikistan, Kyrgyzstan, and China, where the altitude is high, the air column is relatively short, and the atmospheric thickness is thin, so the WVC is low.

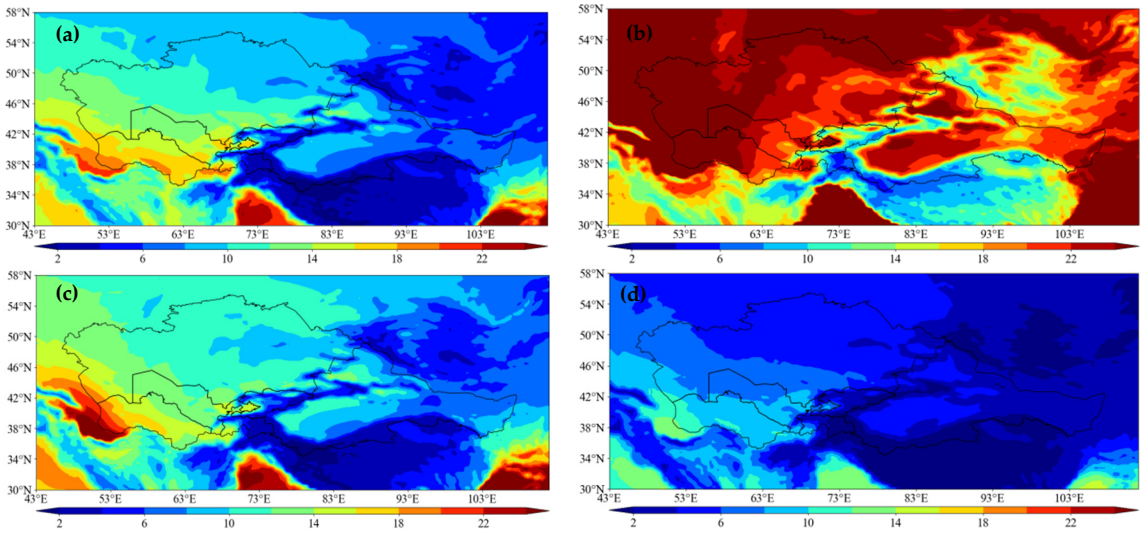

Figure 3. Distribution of seasonal average WVC in arid areas of Central Asia from 1980 to 2019 in (**a**) spring, (**b**) summer, (**c**) autumn, and (**d**) winter (Units: kg·m^{-2}).

3.1.3. Spatial Distribution of the Annual Mean Content of CIWC and CLWC

To understand the distribution of CLWC and CIWC, we calculated CLWC and CIWC from 1980 to 2019 (Figure 4a,b). Therefore, the annual average distribution of CLWC and CIWC was different from that of WVC.

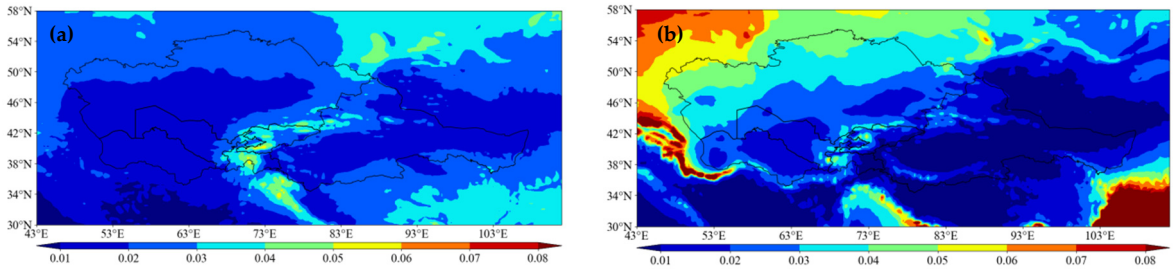

Figure 4. Spatial distribution of CIWC and CLWC in the arid region of Central Asia from 1980 to 2019 (**a**) CLWC; (**b**) CIWC. (Units: kg·m^{-2}).

From 1980 to 2019, the high annual average CLWC zone was mainly located in northwestern Kazakhstan with a maximum value of 0.08 kg·m^{-2} and the low zone was mainly located in Tajikistan, eastern Kyrgyzstan, Xinjiang, China and most of Gansu with a low value of only 0.02 kg·m^{-2}. The annual average maximum of CIWC was located in northern Tajikistan and western Kyrgyzstan, with the maximum value of 0.06 kg·m^{-2}, and the minimum was located in Kazakhstan, Uzbekistan, western Turkmenistan, Xinjiang, and most parts of Gansu, China, with the minimum value of 0.01 kg·m^{-2}.

The contents of CLWC and CIWC in the arid region of central Asia were higher than that in low-altitude areas in spatial distribution. It was larger in the north than in the south as a whole, which is consistent with the topographic distribution characteristics of this area.

3.1.4. Spatial Distribution of Seasonal Contents of CIWC and CLWC

As shown in Figure 5: the distribution regions of maximum and minimum values in each season were the same, showing a large value area in the northwest and a small value area in the southeast. In spring, the maximum CLWC area is located in northern and southern Kazakhstan, including eastern Uzbekistan, with a maximum value of 0.12 kg· m^{-2}, and the minimum area is located in western Kazakhstan, Xinjiang, China, and most of Gansu, with a minimum of only 0.01 kg·m^{-2}. In summer, the maximum CLWC area is distributed in northern Kazakhstan with the highest value of 0.1 kg·m^{-2}, while the

minimum is distributed in most of the arid zone, with the lowest value of 0.02 kg·m^{-2}. In autumn, the cloud water content decreases significantly and the distribution is lower throughout the arid zone, with the minimum value of 0.03 kg·m^{-2}. In winter, the CLWC is lower throughout the arid zone, with the maximum value of 0.02 kg·m^{-2} and CLWC is low throughout the arid zone, reaching a minimum of 0 kg·m^{-2}.

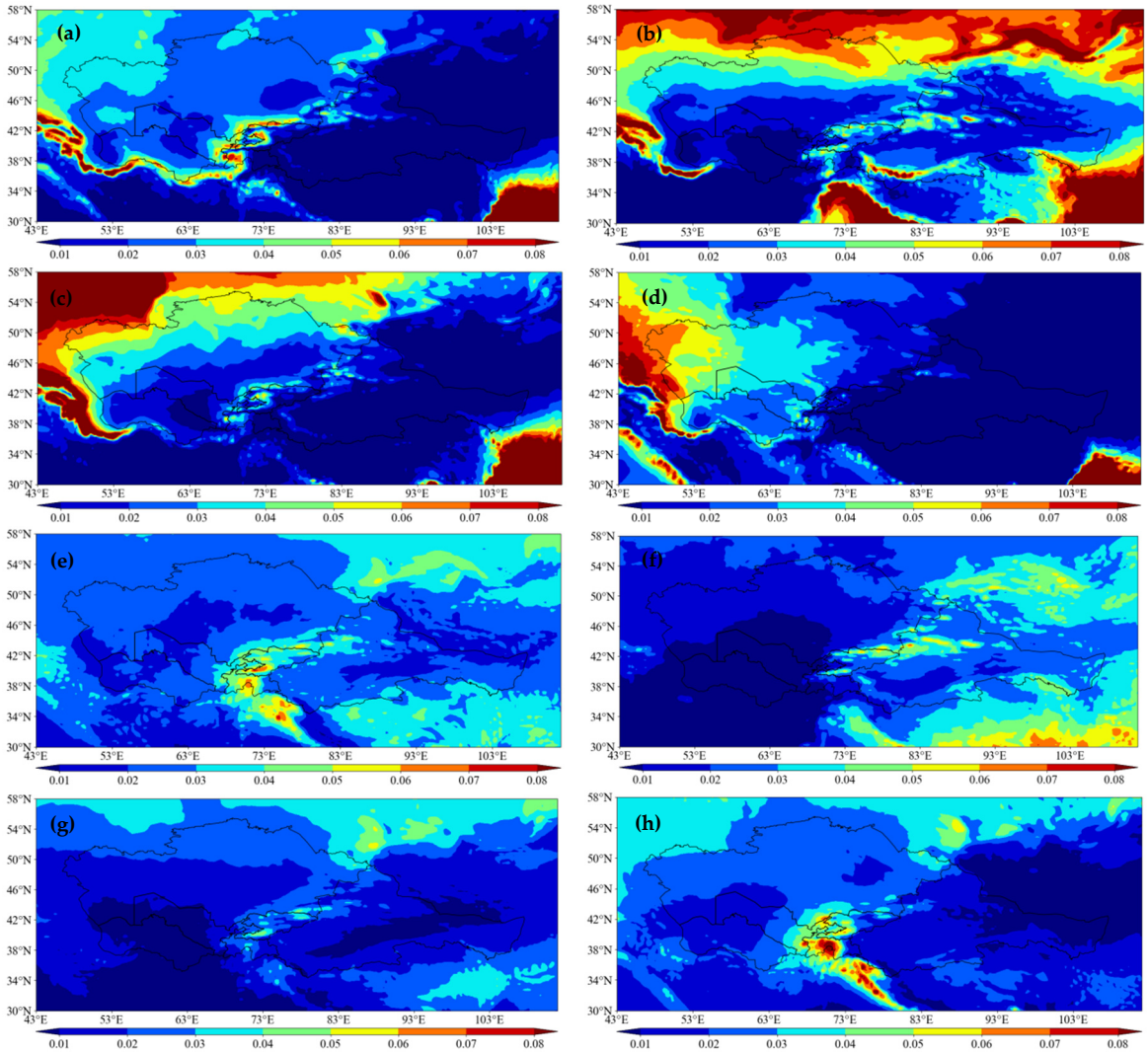

Figure 5. Seasonal average distribution of CLWC and CIWC in arid area of Central Asia from 1980 to 2019 (Units: kg·m^{-2}). Distribution map of cloud water content in an annual average arid area in (**a**) spring, (**b**) summer, (**c**) autumn, and (**d**) winter. Distribution map of CIWC in an annual average arid area in (**e**) spring, (**f**) summer, (**g**) autumn, and (**h**) winter.

The spring CIWC high value zone is located in Tajikistan and Kyrgyzstan, with a maximum of 0.08 kg·m^{-2}, and the low value zone is distributed in most other regions, with a minimum of 0.01 kg·m^{-2}. The summer high value zone is located in northwestern Kazakhstan, with a maximum value of 0.18 kg·m^{-2}, and the minimum value zone is distributed in most other regions, with a minimum value of 0.02 kg·m^{-2}. -The high value in autumn is in the south of Kazakhstan, with a maximum of 0.07 kg·m^{-2}, and the minimum value in western Kazakhstan, western Turkmenistan and Xinjiang, China, with a minimum value of 0.01 kg·m^{-2}. In line with autumn, the high value in winter was distributed in southern Kazakhstan and eastern Uzbekistan, with a maximum of 0.09 kg·m^{-2}, and the minimum in western Kazakhstan, Xinjiang, China, and most of Gansu, with a minimum of 0.01 kg·m^{-2}.

3.2. Time Variation of Atmospheric WVC and Cloud Water Content

3.2.1. Annual Variation of WVC, CIWC and CLWC

The WVC showed an overall upward trend from 1980 to 2019 (Figure 6), equipped with the highest value appearing in 2007, the WVC reaching 12.33 kg·m^{-2}, while the lowest value appearing in 2013, the WVC was 9.904 kg·m^{-2}, and the rest years were stable around 11 kg·m^{-2}.

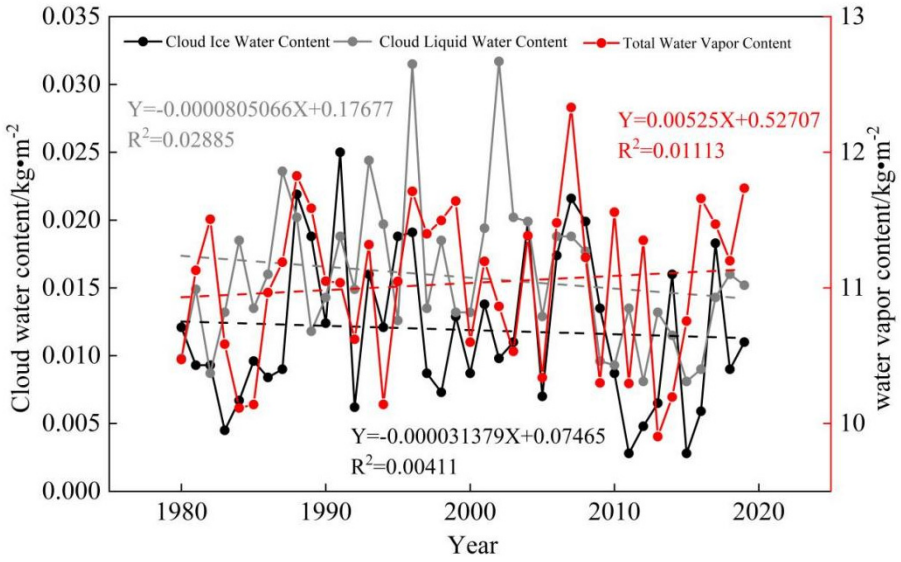

Figure 6. Annual average content variation from 1980 to 2019. (black: CIWV, gray: CLWV, red: WVC).

From 1980 to 2019, in the recent 40 years (Figure 6), the CIWC in the arid region of central Asia showed a declining trend, with a small wave trend. The maximum value appeared in 1993, and the highest value was 0.016 kg·m^{-2}, while the lowest value appeared in 2011, and the lowest value was 0.0028 kg·m^{-2}. The distribution of CLWC shows a downward trend in recent 40 years, with the highest value appearing in 2002 and the highest value being 0.0317 kg·m^{-2}, while the lowest value appeared in 2016 and the lowest value being 0.009 kg·m^{-2}.

3.2.2. Seasonal Variation of WVC, CIWC and CLWC

As seen in the seasonal average graph of WVC (Figure 7), the highest WVC is found in summer, followed by spring and autumn, and the least in winter. WVC showed an increasing trend in spring, with the maximum of 12.198 kg·m^{-2} in 2017 and a minimum of 6.813 kg·m^{-2} in 2003. Summer showed a decreasing trend with an overall high variability, with a maximum of 24.68 kg·m^{-2} in 1989 and a minimum of 17.453 kg·m^{-2} in 2014. Autumn WVC showed an increasing trend with a maximum of 13.318 kg·m^{-2} in 1982 and a minimum of 7.48 kg·m^{-2} in 2003. The autumn WVC showed an increasing trend, with the maximum of 13.318 kg·m^{-2} in 1982 and a minimum of 7.48 kg·m^{-2} in 2003. The winter WVC showed an increasing trend, with the highest in 2019 at 5.62 kg·m^{-2} and the lowest in 2011 at 3.411 kg·m^{-2}.

3.3. Trend Analysis of Atmospheric Water Vapor, CIWC and CLWC

A linear trend analysis and F-test were done for water vapor content, CIWC, and CLWC, and the results were combined to obtain Figure 8, which shows that: Significantly increasing and slightly increasing areas of water vapor content are found in eastern Kazakhstan and northwestern Xinjiang, China, and significantly decreasing areas are found in western and northern Kazakhstan, western Uzbekistan, and western Tajikistan, central and western Kazakhstan, most of Uzbekistan, and Turkmenistan, and a slightly decreasing trend in southwestern Xinjiang, China. Significantly increasing areas of CIWC are found

in southern Xinjiang and Gansu, southeastern and south-western Kazakhstan, most of Kyrgyzstan and northern Turkmenistan showing a slightly increasing trend, and significantly decreasing areas are found in west-central Kazakhstan, Uzbekistan and east-central Turkmenistan, east-central and southwestern Kazakhstan, and west-central Turkmenistan showing a slightly decreasing trend. Significantly increasing areas of CLWC are found in Xinjiang and southern Gansu in China, eastern Xinjiang, and Gansu in China, slightly increasing areas in north-central Kazakhstan, significantly decreasing areas in central-western Kazakhstan and west-central Uzbekistan, eastern Turkmenistan, east-central Kazakhstan, western Xinjiang, and western Turkmenistan in China with a slightly decreasing trend.

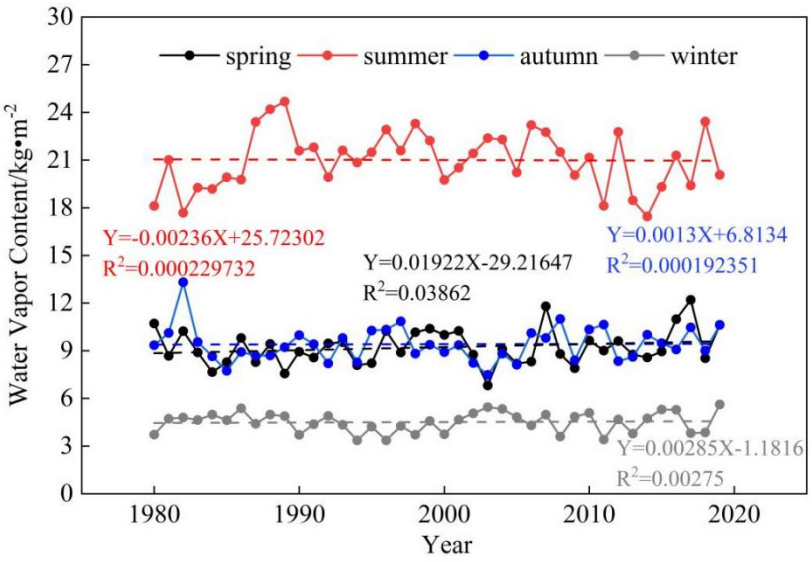

Figure 7. Seasonal average changes of water vapor from 1980 to 2019.

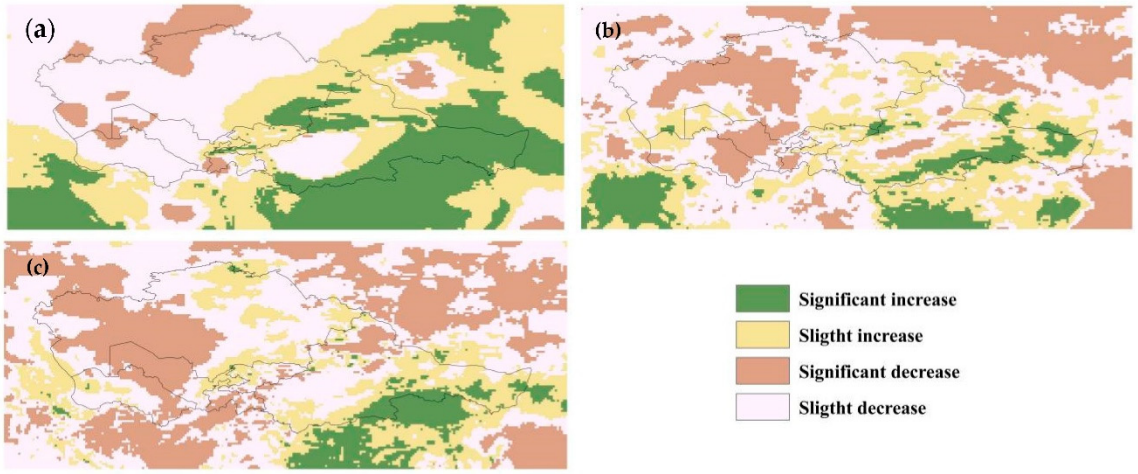

Figure 8. Distribution map of change trend of arid areas in Central Asia from 1980 to 2019 (**a**) WVC, (**b**) CIWC, (**c**) CLWV.

4. Discussion

4.1. Analysis of the Relationship between WVC and Climate Change

Climate change has always been the research focus of the sustainable development of the earth system [21]. Since the 1950s, the warming of the global climate system has accelerated. This observed warming is unprecedented in decades to thousands of years [22]. It can be confirmed that greenhouse gas emissions caused by human activities are the main factor leading to global warming. Since the era of industrialization, global CO_2 emissions

have soared. This forcing caused by human activities has not only led to global warming but also caused a series of other changes in the climate system [23,24]. It is undeniable that the increase of global atmospheric WVC is strongly related to global warming caused by us. From 1980 to 2019, the high-temperature region in the arid region of Central Asia expanded northward from 36° N, most notably in the southwest of the arid region (Figure 9). The IPCC6 report points out that the global land, ocean, and near-surface atmospheric temperatures have accelerated since 1950, and more water vapor growth on land at low latitudes. This is consistent with the distribution of maximum areas of global water vapor observed by us, indicating that global warming has made a disproportionate contribution to the increase of atmospheric WVC. As an important greenhouse gas, the increase of atmospheric WVC will also have an impact on the warming of the global climate system.

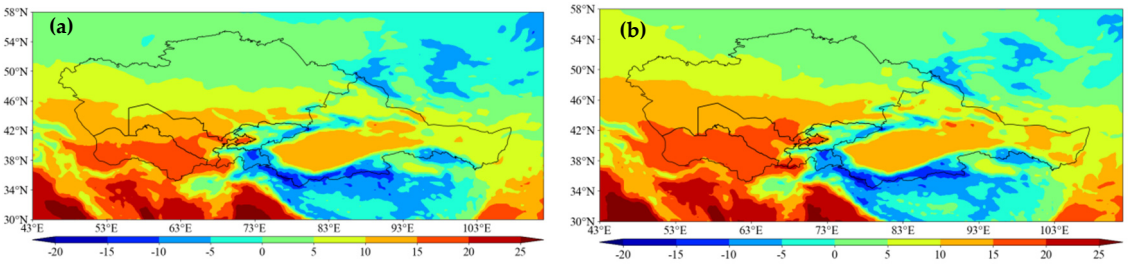

Figure 9. Average temperature distribution in arid areas of Central Asia. (**a**) Average temperature in 1980; (**b**) average temperature in 2019.

4.2. Analysis of Cloud Water Resources in Arid Regions Based on Cloud Cover

As a potential water resource, cloud water resources have the potential value to alleviate the shortage of water resources [25]. The formation process of clouds is mainly formed by condensation or condensation of water vapor in the atmosphere. The formation, evolution, and global distribution of clouds are common result of the interaction of dynamic over-temperature and microphysics processes, which not only determines the change of climate state, such as temperature, water vapor, and precipitation, but also is influenced by some climatic factors [26]. Chen et al. used the ISCCP D2 data set to study cloud cover's temporal and spatial distribution in three different climatic regions in northwest China. The results show the high areas of cloud cover were distributed along the mountains in Northwest China, and the formation of clouds was influenced by complex topography. Even in the same climate zone, the cloud cover varied greatly [27].

Figure 10a is the annual average spatial distribution of total cloud cover in the arid region from 1980 to 2019. It can be seen that the total cloud cover in northern Kazakhstan and northern Xinjiang of China was significantly higher than in other regions. This region is affected by water vapor from Siberia Plain, and when it confronts the mountains, the windward slope airflow rises to form higher cloud cover [28]. According to the comparison of the spatial distribution of high, medium, and low cloud cover with the Annual average CLWC and CIWC (Figure 4), the results show that the distribution characteristics of high cloud cover and CLWC and CIWC are inconsistent, and the influence of high cloud cover on them is not obvious. The distribution characteristics of medium cloud cover and low cloud cover are high in the north and middle of the arid area, and low in the southwest and east, which are consistent with the distribution characteristics of CLWC and CIWC. Therefore, the influence of medium and low cloud amounts on CLWC and CIWC is obvious. Cloud cover is closely related to the content of CLWC and CIWC. Therefore, the research on cloud cover and cloud water resources is of great strategic significance for the rational and full development and utilization of cloud water resources in arid areas and for ensuring the safety of regional water resources.

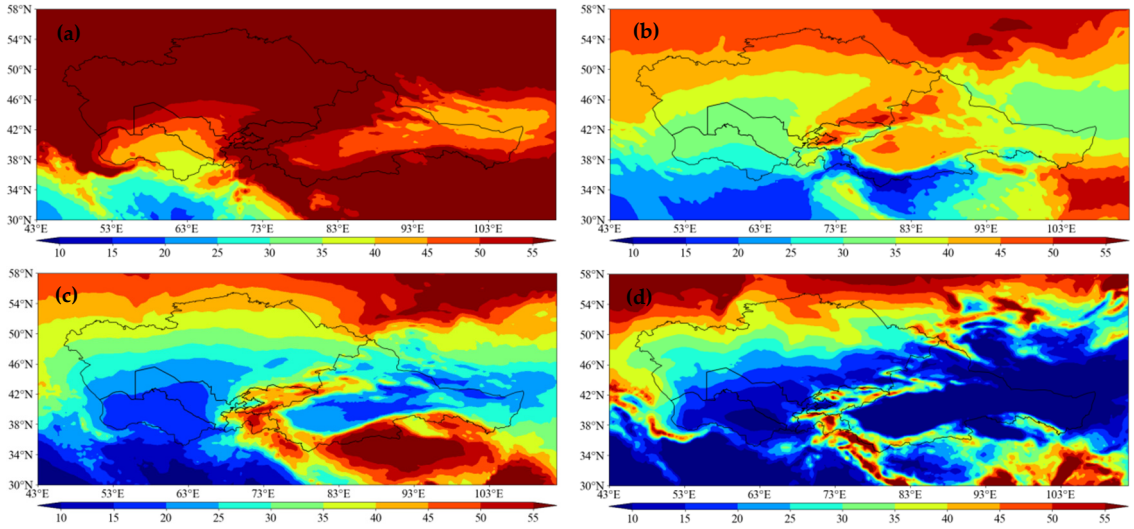

Figure 10. Annual average spatial distribution of total, high, medium, and low cloud cover in arid regions of central Asia from 1980 to 2019. (Units:"0–1") (**a**) TCC, (**b**) HCC, (**c**) MCC, (**d**) LCC.

5. Conclusions

(1) From 1980 to 2019, the annual average WVC in the arid region of central Asia increased, while the annual average CLWC and the annual average CIWC decreased.

(2) The high-value areas of the annual average distribution of WVC in the arid area of Central Asia are mainly concentrated in flat areas such as plains, which are distributed in the southwest of Turkmenistan, and distributed between 22 and 26 kg·m^{-2}. Low-value areas were concentrated in high-altitude areas, such as the plateau, distributed in Tajikistan, Kyrgyzstan, and western Xinjiang of China, distributed between 2 and 8 kg·m^{-2}. The distribution characteristics of the annual average WVC in four seasons were the same as the annual average distribution, which was high in the west and low in the east.

(3) The annual average CLWC and CIWC results is the high value of CLWC in the arid zone of Central Asia was in northwestern Kazakhstan with the maximum value of 0.08 kg·m^{-2}; the minimum value was distributed in Tajikistan, eastern Kyrgyzstan, Xinjiang, and Gansu, and the lowest value was only 0.02 kg·m^{-2}. The distribution characteristics of CLWC in the four seasons in the arid region were high in the northwest and low in the southeast, while the CIWC in the four seasons in the arid region was high in the middle and low on both sides.

Author Contributions: Conceptualization, G.Z. and K.Z.; methodology, J.L.; software, L.W. and L.S.; validation, Y.L.; formal analysis, Y.X.; writing-original draft preparation, K.Z.; writing-review and editing, K.Z.; visualization, X.L.; supervision, Y.J.; data curation, W.Z. and L.Y. All authors have read and agreed to the published version of the manuscript.

Funding: This research was funded by the National Natural Science Foundation of China (41867030, 41971036), National Natural Science Foundation innovation research group science foundation of China (41421061). The authors greatly thank you for the support of the above funds.

Institutional Review Board Statement: Not applicable.

Informed Consent Statement: Not applicable.

Data Availability Statement: The data that support the findings of this study are available on request from the corresponding author. TCWV, CLWV, CIWV, TP, TCC, HCC, MCC, LCC can be obtained at the European Mid-range Weather Forecast Center (https://cds.climate.copernicus.eu/cdsapp#!/yourrequests?tab=form, accessed on 1 May 2022).

Conflicts of Interest: The authors declare no competing interests.

References

1. Guiot, J.; Cramer, W. Climate change: The 2015 Paris Agreement thresholds and Mediterranean basin ecosystems. *Science* **2016**, *354*, 465–468. [CrossRef] [PubMed]
2. Zeng, S.K.; Yong, B. Evaluation of the GPM-based IMERG and GSMaP precipitation estimates over the Sichuan region. *Acta Geogr. Sin.* **2019**, *74*, 1305–1318.
3. Li, X.; Guo, X.; Zhu, J. Climatic distribution features and trends of cloud water resources over China. *Chin. J. Atmos. Sci.* **2008**, *32*, 1094–1106.
4. Donat, M.G.; Lowry, A.L.; Alexander, L.V.; O'Gorman, P.A.; Maher, N. More extreme pre-cipitation in the world's dry and wet regions. *Nat. Clim. Chang.* **2016**, *6*, 508–513. [CrossRef]
5. Fang, J.; Zhu, J.; Shi, Y. The responses of ecosystems to global warming. *Sci. Bull.* **2018**, *63*, 136–140. [CrossRef]
6. Cao, L.; Yu, J.; Ge, Z. Water vapor content in the atmosphere and its variation trend over North China. *Adv. Water Sci.* **2005**, *16*, 439–443.
7. Chen, Y.; Deng, J. Vertical Distribution of Ice Water Content in Clouds during Heavy Rains around Tianshan Mountain. *Resour. Sci.* **2013**, *35*, 655–664.
8. Howard, K.; Howard, K.K. The new "Silk Road Economic Belt" as a threat to the sustainable management of Central Asia's transboundary water resources. *Environ. Earth Sci.* **2016**, *75*, 976. [CrossRef]
9. Chen, X. *Retrieval and Analysis of Evapotranspiration in Central Areas of Asia*; Meteorogical Press: Beijing, China, 2012.
10. Chen, X.; Jiang, F.Q.; Wang, Y.J.; Li, Y.M.; Hu, R.J. Characteristics of the Eco-geographical Pattern in Arid Land of Central Asia. *Arid. Zone Res.* **2013**, *30*, 385–390.
11. Heng, Z.; Fu, Y. Analysis of global cloud, water, cloud and ice climate distribution based on NCEP CFSR data. In Proceedings of the 28th Annual Meeting of China Meteorological Society-S4: Addressing Climate Change and Developing Low-Carbon Economy, Xiamen, China, 2 November 2011.
12. Kawase, H.; Takeuchi, Y.; Sato, T.; Kimura, F. Precipitable Water Vapor around Orographically Induced Convergence Line. *Sola* **2006**, *2*, 25–28. [CrossRef]
13. Smith, B.L.; Yuter, S.E. Water Vapor Fluxes and Orographic Precipitation over Northern California Associated with a Landfalling Atmospheric River. *Mon. Weather. Rev.* **2010**, *138*, 74–100. [CrossRef]
14. Giovannettone, J.P.; Barros, A.P. Probing Regional Orographic Controls of Precipitation and Cloudiness in the Central Andes Using Satellite Data. *J. Hydrometeorol.* **2009**, *10*, 167–182. [CrossRef]
15. Qian, Z.; Wu, T.; Liang, X. Feature of Mean Vertical Circulation over the Qinghai-Xizang Plateau and Its Neighborhood. *Chin. J. Atmos. Sci.* **2001**, *25*, 444–454.
16. Gaffen, D.J.; Elliott, W.P.; Robock, A. Relationships between tropospheric water vapor and surface temperature as observed by radiosondes. *Geophys. Res. Lett.* **2013**, *19*, 1839–1842. [CrossRef]
17. Balsamo, G.; Albergel, C.; Beljaars, A.; Boussetta, S.; Brun, E.; Cloke, H.; Dee, D.; Dutra, E.; Muñoz-Sabateret, J.; Pappenberger, F.; et al. ERA-Interim/Land: A global land surface reanalysis data set. *Hydrol. Earth Syst. Sci.* **2015**, *19*, 389–407. [CrossRef]
18. Hu, R. *Physical Geography of the Tianshan Mountains in China*; Beijing; China Environmental Science Press: Beijing, China, 2004.
19. Balashova, Y.; Zhitomirskaya, O.; Semyonova, O. *Climatologic Characterization of the Central Asian Republics*; Hydrom-Eteorological Publishing: Leningrad, Russia, 2006.
20. Li, G.; Huang, D.; Guo, J. *Ground-Based Gps/Met*; Science Press: Beijing, China, 2010; pp. 148–150.
21. Rubel, F.; Kottek, M. Observed and projected climate shifts 1901–2100 depicted by world maps of the Köppen-Geiger climate classification. *Meteorol. Z.* **2010**, *19*, 135–141. [CrossRef]
22. IPCC. 2022: Summary for Policymakers. In *Climate Change 2022: Impacts, Adaptation, and Vulnerability. Contribution of Working Group II to the Sixth Assessment Report of the Intergovernmental Panel on Climate Change*; Pörtner, H.-O., Roberts, D.C., Poloczanska, E.S., Mintenbeck, K., Tignor, M., Alegría, A., Craig, M., Langsdorf, S., Löschke, S., Möller, V., et al., Eds.; Cambridge University Press: Cambridge, UK, 2022; in press.
23. Burrows, M.T.; Schoeman, D.S.; Buckley, L.B.; Moore, P.; Poloczanska, E.S.; Brander, K.M.; Brown, C.; Bruno, J.F.; Duarte, C.M.; Halpern, B.S.; et al. The pace of shifting climate in marine and terrestrial ecosystems. *Science* **2011**, *334*, 652–655. [CrossRef]
24. Zhao, H.; Xu, Z.; Zhao, J.; Huang, W. A drought rarity and evapotranspiration-based index as a suitable agricultural drought indicator. *Ecol. Indic.* **2017**, *82*, 530–538. [CrossRef]
25. Du, L.; Li, J. Analysis on Cloud and Vapor Flux in the Northeast of the Qinghai—Tibet Plateau during the Period from 2001 to 2011. *Arid. Zone Res.* **2012**, *29*, 862–869.
26. Geiss, A.; Marchand, R.; Thompson, L. The Influence of Sea Surface Temperature Reemergence on Marine Stratiform Cloud. *Geophys. Res. Lett.* **2020**, *47*, e2020GL086957. [CrossRef]
27. Chen, Y.H.; Huang, J.P.; Chen, C.H.; Zhang, Q.; Feng, J.D.; Jin, H.C.; Wang, T.H. Temporal and Spatial Distributions of Cloud Water Resources over Northwestern China. *Plateau Meteorol.* **2005**, *24*, 905–912.
28. Wang, H.Q.; Chen, Y.H.; Peng, K.J. Study on Cloud Water Resources of Mountain Ranges in Xinjiang Base on Aqua Satellite Date. *J. Nat. Resour.* **2011**, *26*, 89–96.